Spring Transition Period in Lake Ontario — A Numerical Study of the Causes of the Large Biological and Chemical Gradients[1]

DONALD SCAVIA AND JOHN R. BENNETT

Great Lakes Environmental Research Laboratory, National Oceanic and Atmospheric Administration, Ann Arbor, MI 48104, USA

SCAVIA, D., AND J. R. BENNETT. 1980. Spring transition period in Lake Ontario — a numerical study of the causes of the large biological and chemical gradients. Can. J. Fish. Aquat. Sci. 37: 823–833.

A two-dimensional model that calculates physical transport, as well as in situ biological and chemical transformations, accurately simulates observations made along a north–south transect in Lake Ontario during April–June 1972. Simulation results show that, during the transition period between spring and summer, the inshore–offshore structure of biological and chemical distributions is controlled by the interaction of in situ processes and differences in vertical mixing on either side of the 4° isotherm. Owing to reversals in flow patterns, the effect of advection is to reduce concentration gradients, but the effect on overall distributions is minimal. An analysis of sinking losses in one- and two-dimensional models indicates that the artificially low sinking rates used in one-dimensional models of the Great Lakes result from the neglect of upwelling.

Key words: Lake Ontario; model, hydrodynamic, ecological; sinking, upwelling, convection cells, chemical distributions

SCAVIA, D., AND J. R. BENNETT. 1980. Spring transition period in Lake Ontario — a numerical study of the causes of the large biological and chemical gradients. Can. J. Fish. Aquat. Sci. 37: 823–833.

Un modèle à deux dimensions calculant le transport physique ainsi que les transformations biologiques et chimiques in situ simule avec précision les observations effectuées le long d'une coupe nord-sud du lac Ontario entre avril et juin 1972. Les résultats de cette simulation démontrent que, durant la période de transition printemps–été, la structure, du rivage vers le large, des distributions biologiques et chimiques est réglée par l'interaction de processus in situ et de différences de mélange vertical de part et d'autre de l'isotherme de 4°. Par suite d'inversions de la circulation, l'effet de l'advection est de réduire les gradients de concentration, mais l'effet d'ensemble sur les distributions est minimale. L'analyse des pertes par plongée des eaux dans des modèles à une et deux dimensions indique que les taux de plongée artificiellement bas utilisés dans les modèles à une dimension des Grands Lacs résultent du fait qu'on ne tient pas compte de la remontée d'eaux profondes.

Received August 23, 1979
Accepted January 25, 1980

Reçu le 23 août 1979
Accepté le 25 janvier 1980

THE spatial distribution of biological and chemical properties in the Great Lakes is determined by variations of water depth, sunlight, and temperature; by the locations of rivers; and by currents. Separating these physical factors from in situ transformations is a difficult problem, a problem which numerical simulation can help solve.

Stadelmann and Fraser (1974) described seasonal variations in nitrogen and phosphorus and proposed a simple nutrient cycle model to describe biological/chemical processes in the summer — average epilimnion along a north–south transect of Lake Ontario. However, they did not examine detailed hydrodynamic effects. Using a three-dimensional simulation, Simons (1976a) examined the importance of physical processes in Lake Ontario. He found vertical mixing to be more important than currents in spring, but currents to be dominant in summer and fall. But, he did not compare the physical with the biological/chemical processes. We will do that here.

We choose to focus on the transition period between spring and summer because both vertical mixing and large-scale circulation are important. In addition, if we limit ourselves to this period, the temperature and current patterns of Lake Ontario are relatively two-dimensional (i.e. small longshore gradients). We can therefore make the assumption that variations along the long axis of the lake are negligible. Here we simulate the flow, temperature, biology, and chemistry for a north–south transect of the lake. Our approach is as follows.

The temperature calculations of a hydrodynamic model (Bennett 1971, 1974) were compared to ob-

[1]GLERL contribution No. 134.

Printed in Canada (J5752)
Imprimé au Canada (J5752)

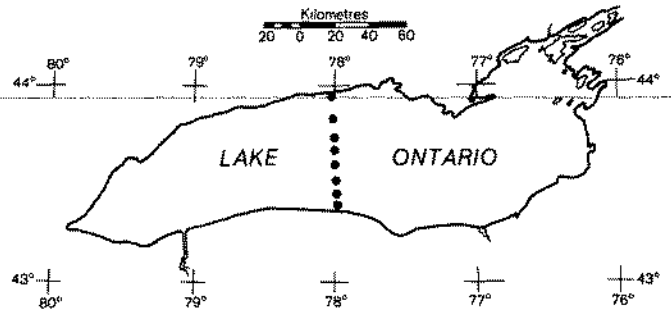

FIG. 1. Lake Ontario showing location of sample stations along the north–south transect under investigation.

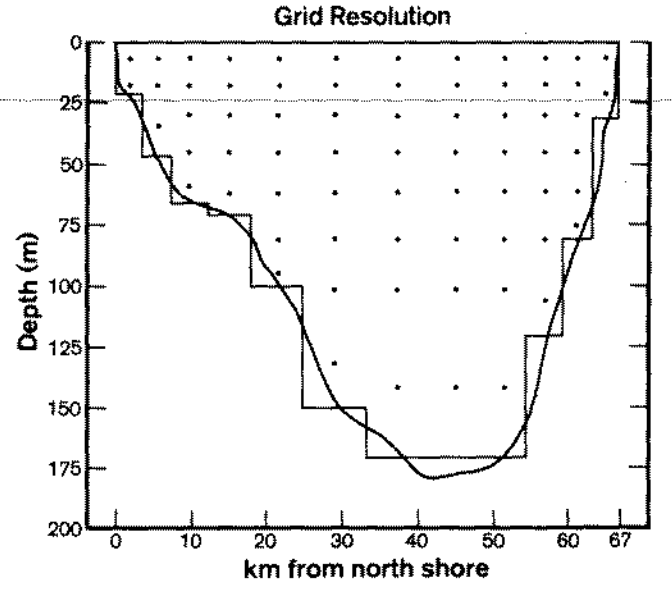

FIG. 2. Lake Ontario, north–south transect, two-dimensional model grid. Transect is approximately along 78°W longitude. Dots represent centers of model grid boxes.

servations, and the model was adjusted until computed and observed temperature contours were in general agreement. We then repeated the calculations, this time including the chemical and biological processes from an ecological model (Scavia et al. 1976; Scavia 1980), and compared them to observations. Only the sinking rate in the ecological calculations was adjusted to obtain good agreement between computed and observed variables.

In the remaining sections of this paper we will describe the transect data and model input for the hydrodynamic and ecological models, compare the observations with the model, and then analyze the effects of sedimentation and transport versus in situ processes.

Data and Models

Data used in this study were collected during the International Field Year for the Great Lakes (IFYGL) in 1972–73. Observations of temperature, nutrients, and biomass variables for our study were obtained from STORET, the data management system of the U.S. Environmental Protection Agency, and are based on collections made by the Canada Centre for Inland Waters (Stadelmann and Fraser 1974). The north–south transect used here follows approximately the 78°W longitude (Fig. 1) and has eight stations with between 5 and 10 depths sampled at each. A total of nine cruises was conducted, but we will analyze only the spring warming period: three cruises conducted during April 12–14, May 24–26, and June 20–22. Methods of data collection and measurement can be found in Stadelmann and Fraser (1974), Stadelmann and Munawar (1974), and Vollenweider et al. (1974).

Input data for the model include solar radiation and photoperiod (percent sunlit day) for phytoplankton calculations and heat flux and wind stress for hydrodynamic calculations. Incident solar radiation varied between 160 and 320 W/m^2 and was input as weekly averages from Atwater and Ball (1974). Photoperiod varied between 52 and 64% of the day.

The hydrodynamic model is driven by lake-averaged values of wind stress and net heat flux. The wind stress was calculated from all available IFYGL meteorological buoys with a wind stress coefficient (the product of a drag coefficient and the air–water density ratio) of 2.5×10^{-6}. We used the heat flux estimates Boyce (1975) made from lake temperature measurements as did Simons (1976a, b). The coefficients of vertical viscosity and diffusion are a constant value, 32 cm$^2 \cdot$s^{-1}, modified by the Munk–Anderson functions of the Richardson number. But, when density decreases with depth the diffusion coefficient is increased to a value large enough that temperature and all ecological parameters are vertically mixed. Model calculations were performed with a time step of 2 h along a stretched grid (Fig. 2) that emphasizes resolution of the nearshore and surface. This grid is coarse, but we repeated the calculations using one half the grid size in both directions and found only small differences.

The ecological framework of this model was developed previously for simulation and analysis of a two-layer, lake-wide-averaged Lake Ontario system (Scavia et al. 1976; Scavia 1980). The crude physical segmentation in this previous work was intentional; it reduced the complexity of physical processes and allowed investigations with emphasis on biological, chemical, and simple physical processes at a lake-wide-averaged scale. Ecological calculations performed within the present physical context are the same as those calculated for the cruder segmentation. Detailed documentation of the system equations, demonstration of the ability of the model to simulate lake-wide average conditions, and examination of biological and chemical processes on that scale can be found in Scavia (1979, 1980). What follows are general descriptions

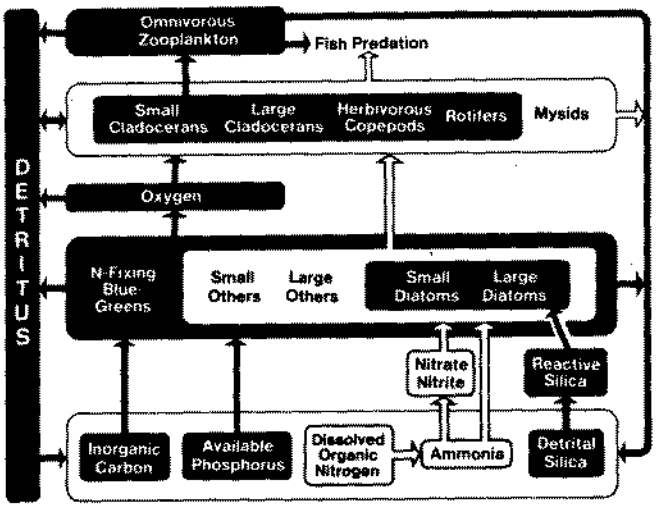

FIG. 3. Components of the ecological portion of the model (from Scavia 1980). Arrows indicate flow of carbon, phosphorus, nitrogen, and silica.

of the biological and chemical processes included in the model.

The ecological portion of the model (Fig. 3) predicts phytoplankton, zooplankton, cycles of phosphorus, nitrogen, silicon, and carbon, and oxygen balance; and calculations of carbonate equilibrium. Each model compartment is represented by a differential equation for the biological and chemical processes. For example, the phytoplankton equation includes terms for gross primary production, respiration, excretion, grazing, and sinking; and the zooplankton equation includes terms for grazing assimilation, respiration, excretion, defecation, and predation.

Gross phytoplankton production is considered a single-step process that assumes that, for the time scale of the modeled processes, rates of uptake and growth are in equilibrium. The process is modeled with a temperature-dependent maximum growth rate times a reduction factor for light- and nutrient-limitation. Potential light-limitation is modeled after Vollenweider (1965) and Steele (1965) and potential nutrient-limitation is expressed as a Michaelis–Menten term for each nutrient. The threshold formulation is used to determine overall limitation. Phytoplankton respiration is considered to be the sum of a low maintenance rate plus a term proportional to production and temperature. To maintain constant nutrient stoichiometry within the plankton, we set nutrient excretion proportional to respired carbon.

Zooplankton grazing is handled as a temperature-dependent saturation expression based on total food supply. The expression includes a minimum threshold for feeding as well as resource partitioning based on size selection. Feeding and assimilation efficiencies are regarded as food-specific constants. Food ingested but not assimilated is egested as detritus. Respiration is a temperature-dependent process that is the sum of a low maintenance rate and a term proportional to the feeding rate. Nutrient excretion is proportional to respiration.

Transformation rates between detritus, dissolved organic nitrogen, ammonia, nitrite plus nitrate, available phosphorus, and available silicon pools all are temperature-dependent and first-order. Sinking rates of phytoplankton and detritus are size- and density-dependent.

Results

Physical Properties

During the spring transition period a combination of strong heating and low wind speeds causes the thermocline to form. Because the lake begins the spring colder than 4°C, the temperature of maximum density, this process starts in the shallow water. Thus, the lake is divided into two hydrodynamic regimes — a deep region where the water temperature is less than 4°C and where surface heating causes vertical mixing, and a shallow region near the coast with temperature greater than 4°C, which may stratify.

In Fig. 4 the simulated temperature is compared with observations. The model correctly simulates this general spring temperature pattern and the depth of the thermocline. In addition, the fact that the thermocline extends further off the north shore than the south is also reproduced. There are two reasons for this: the north shore is shallower than the south and for the last 3 wk of the simulation the wind was from the west, causing upwelling on the north shore and downwelling on the south shore.

Wind and buoyancy combine to cause simple but interesting flow patterns. The wind tends to drive a one-cell pattern, with upwelling at the shore to the left of the wind and downwelling near the opposite shore. Heating drives a two-cell pattern, with the warm water rising near both shores and colder water sinking in the deep region.

Figure 5 shows the mean circulation for three, 24-d periods and the mean for the entire 72-d simulation. During the first two 24-d periods the wind came predominantly from the east; because the Coriolis force deflects the water to the right, the water near the surface flows north and the deep water flows south in compensation. Upwelling near the south shore and downwelling near the north shore closes this circulation. During the last 24-d period the wind and circulation reverse. For the whole 72-d period the wind's effects tend to cancel and the circulation looks like the thermally driven pattern.

This simple picture of a combination of wind and buoyancy effects should be considered an average circulation pattern. At any given time the flow is dominated by the wind, and it is only because the thermally driven flow is more persistent that it is as important as the wind-driven flow. The average longshore flow, generated

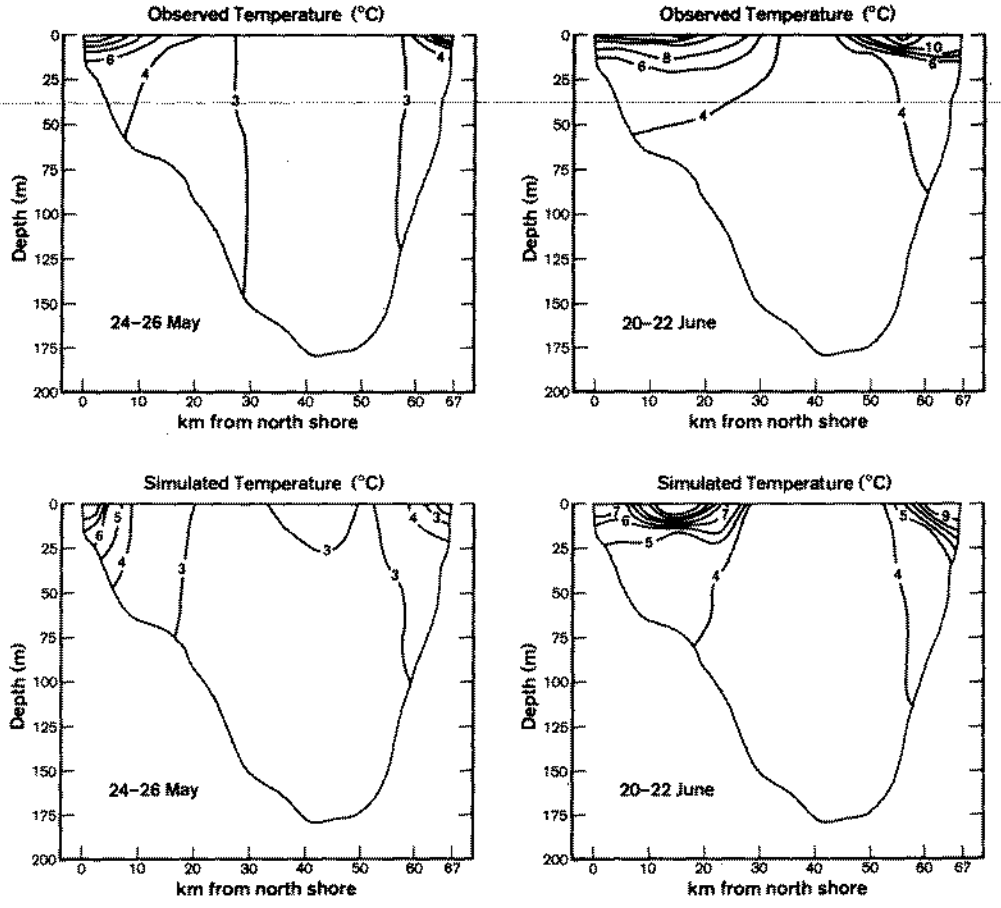

FIG. 4. Comparison of observed (*upper*) and calculated (*lower*) temperatures (°C) corresponding to May and June cruises.

by the Coriolis force, is cyclonic, to the east along the south shore and to the west along the north shore.

ECOLOGICAL PROPERTIES

Using the ecological equations and parameters unchanged from the original lake-wide-average, two-layer version resulted in comparisons between observations and computations that were generally good for plant nutrients (phosphorus, nitrogen, silica) but poorer for estimates of biomass (chlorophyll *a*, particulate organic carbon). By the end of the simulation period, model estimates of biomass in the nearshore surface areas were 1.5 to 2.5 times higher than observations (about June 20). We increased the average phytoplankton sinking rate by one order of magnitude over that used in the simple two-layer model, from ~0.05 to 0.5 $m \cdot d^{-1}$. This resulted in better agreement between observations and calculations. This simple modification improved the simulation of both nutrients and biomass variables.

In general, nutrient concentrations had slight offshore gradients and were vertically homogeneous in early April. These data were used to initiate the simulation. By the end of May, distinct offshore gradients had developed: nutrients, especially phosphorus and silica, were severely depleted in the regions within 10 km of both shores (Fig. 6). Also, at this time, no strong vertical gradients were obvious in either the model output or the data. At the end of the period of simulation (corresponding to the June 20–22 cruise) the symmetry of the north- and south-shore contours was lost. The region of nutrient depletion along the north increased to greater than 25 km and vertical stratification was not as strong there. The spatial and temporal progression of the region of nutrient depletion is demonstrated for phosphorus in Fig. 6; inorganic nitrogen and soluble reactive silica have similar patterns. The comparison between observed total dissolved phosphorus (TDP) and modeled available phosphorus (AP) is made because previous simulations of phosphorus cycling in Lake Ontario (Scavia 1980) indicated that in spring AP is approximated best by TDP, due, presumably, to production of easily hydrolyzed phosphorus compounds during the previous winter.

Biomass parameters (chlorophyll *a* and particulate organic carbon) in April were relatively homogeneous

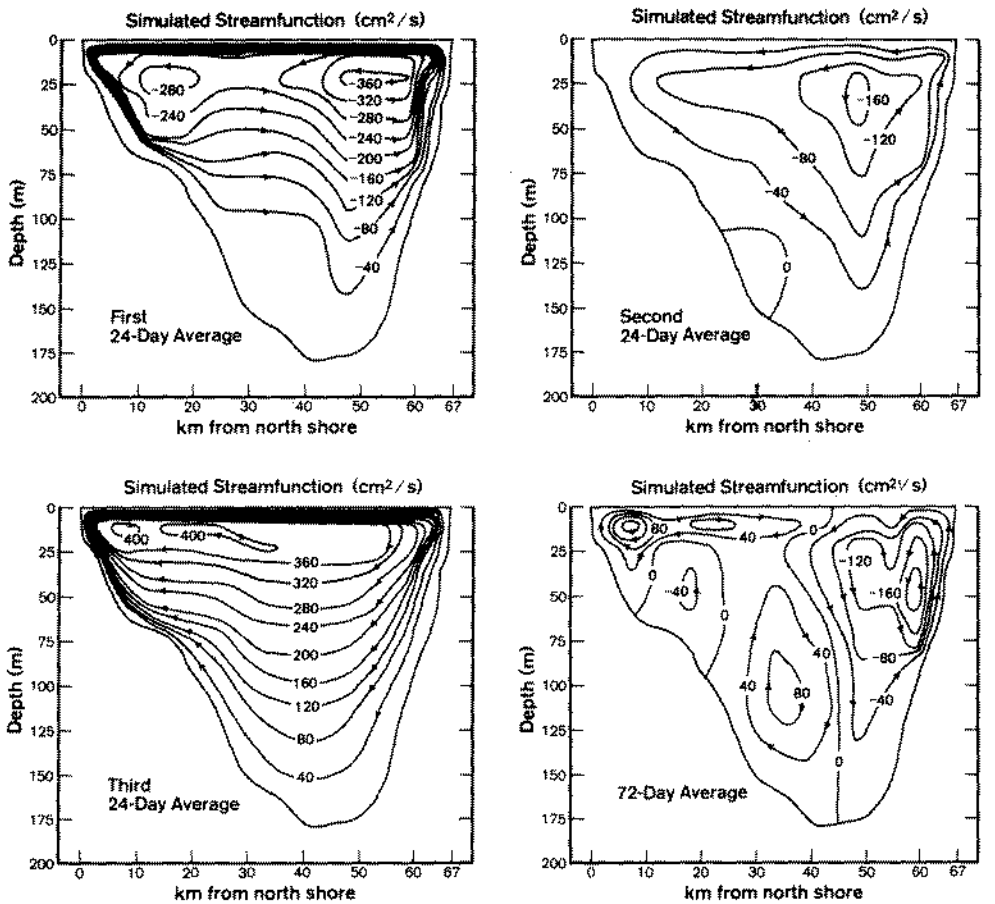

FIG. 5. Contours of calculated stream functions (cm²/s) averaged over three 24-d periods and over the entire period of simulation.

vertically, with higher values nearshore. Patterns in May generally showed offshore gradients and little vertical structure (Fig. 7), except for evidence of nearshore subsurface chlorophyll peaks, which the model did not reproduce. The simulations indicated that between the May and June cruises, upwelling moved the higher nearshore concentrations offshore, creating a lens of high biomass about 15 km from the north shore. (See Fig. 4, 5). By the time of the June cruise, increased nearshore production apparently created higher biomass again close to shore. A similar structure was produced along the south shore with the exception that, like the nutrient contours, the biomass contours were constrained closer to shore by the wind-driven flow.

Discussion

In the analysis of the progression and simulation of nutrient and biomass isopleths, two important considerations became clear: (1) the impact of sinking on biomass and the formulation of that process in various models: (2) the relative influence of physical transport versus in situ processes. These are discussed below.

SINKING

Parameterization of plankton sedimentation in models of the Great Lakes' ecosystems has proved difficult. Sinking rates used in these models have had to be considerably lower than rates measured in laboratory studies. Sinking rates of algae, within typical size ranges of Lake Ontario plankton (Stoermer and Ladewski 1978), are summarized in Table 1. From available information one would expect the free-fall settling rates for Lake Ontario phytoplankton to be within 0.4–1.2 $m \cdot d^{-1}$. It has been recognized (e.g. Thomann et al. 1975; Scavia 1980) that sinking rates used in one- or two-layer, horizontally averaged Great Lakes' models (Table 2) are considerably lower than rates measured under quiescent laboratory conditions; however, if these measured sinking rates were used in the calculations, loss rates from the upper mixed layer would be too great to allow sufficient net biomass production in the models. Rates 10 or 20 times lower are required to obtain better agreement between observations and calculations of both phytoplankton standing crops and total nutrient loss to the sediment (Scavia 1980; DiToro and Matystik 1979).

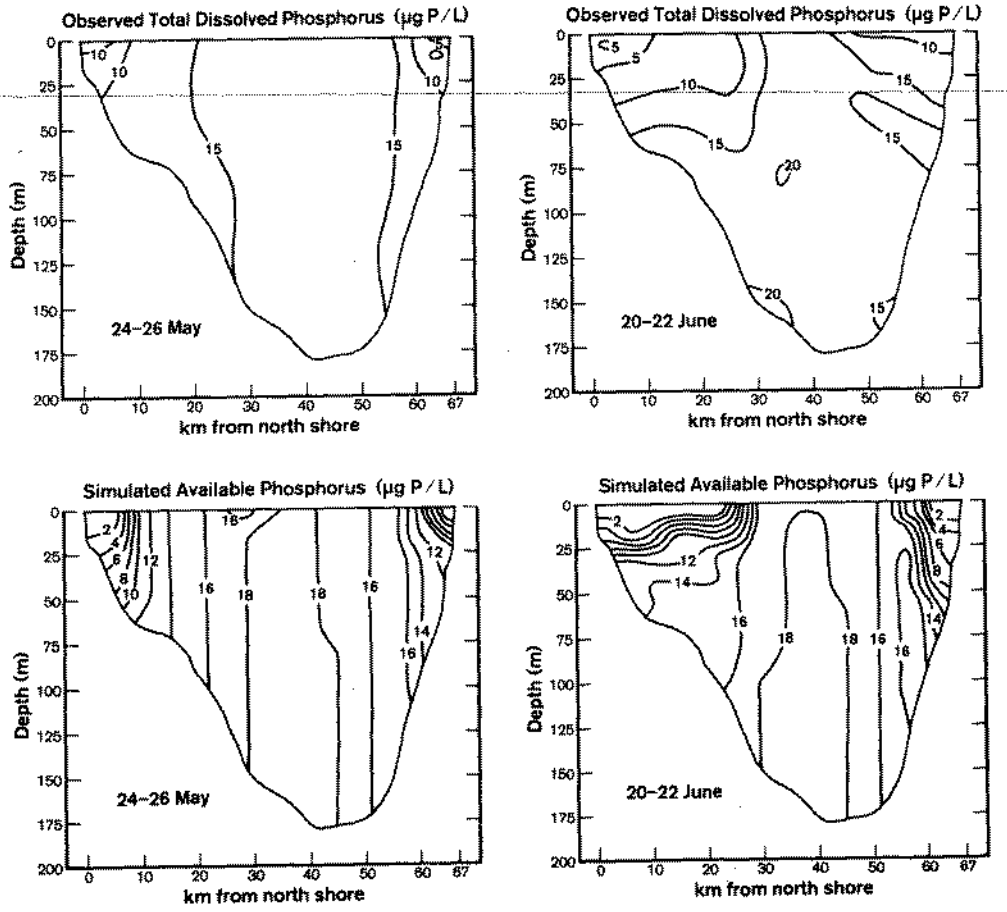

FIG. 6. Comparison of observed (*upper*) and calculated (*lower*) concentrations of phosphorus (μg P/L) corresponding to May and June cruises. Observed phosphorus is total dissolved phosphorus and calculated phosphorus is that considered available for phytoplankton growth.

As discussed above, the transect model required use of more realistic sinking rates ($0.5\ m \cdot d^{-1}$). Using the typical "one-dimensional" sinking rates ($0.05\ m \cdot d^{-1}$) resulted in poorer agreement between observations and calculations. In fact, there was little difference between using a rate of $0.05\ m \cdot d^{-1}$ and eliminating sinking entirely.

To explore the reasons for the discrepancies between measured sinking rates, rates used in one-dimensional models, and rates used in the present work, we examined some of the important phenomena that can affect sinking: physiological state, shape, size, colony formation, and water movements. Sinking rates appear to vary with physiological state only by factors of 2–4 (Titman and Kilham 1976; Smayda 1970, 1974; Eppley et al. 1967). Typical shape corrections for Stokes settling of nonspherical particles are at most a factor of 2 (McNown and Malaika 1950; Hutchinson 1967). Size and colony formation also are not sufficient to account for the reduced rates.

For water movements to affect particle sedimentation significantly, there must be a correlation between areas of upwelling and high biomass concentrations. The correlation would result in a net upward transport of particulates and would consequently require lower sinking rates in one-dimensional models, which cannot account explicitly for such vertical water movements. Although the wind-driven circulation in our two-dimensional model produces upwelling and downwelling on opposite shores (Fig. 5a–c), the composite average circulation over the entire period of simulation (Fig. 5d) has rising motion on both shores. These areas of net upwelling are in fact associated with areas of higher biomass concentrations (Fig. 7) and thus one would expect a net upward transport opposing sedimentation.

The association of higher biomass concentrations and these nearshore zones may be partially explained by plankton responses to higher nearshore temperatures, to higher rates of nutrient supply in the nearshore upwelling zones, or to some other fortuitous set of phenomena that may not persist beyond this particular spring transition period.

Another cause for higher plankton concentrations

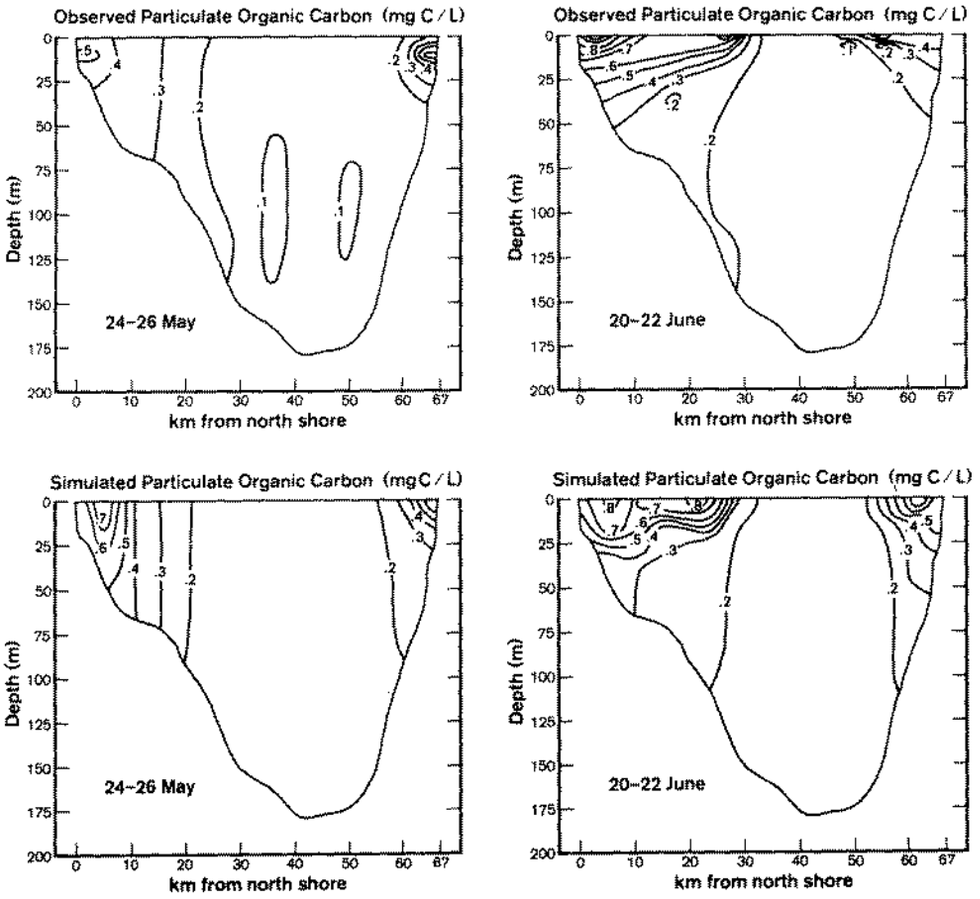

FIG. 7. Comparison of observed (*upper*) and calculated (*lower*) concentrations of particulate organic carbon (mg C/L) corresponding to May and June cruises. Calculated carbon is the sum of simulated phytoplankton, zooplankton, and detrital carbon.

in these nearshore zones may be entrapment of particles within zones of retention of large-scale convection cells set up during upwelling. This phenomenon has been discussed often with regard to Langmuir circulation (e.g. Stommel 1949; Smayda 1970; Titman and Kilham 1976); however, the grid of our model cannot resolve this smaller-scale circulation. If the larger-scale vertical circulation patterns predominant in our study are analogous to Langmuir cells, then their effects on sinking can be estimated.

Titman and Kilham (1976) demonstrated the difference in sinking loss rates calculated by using a simple algebraic relationship (Table 3, Eq. 1) and by using an estimate of loss from a Langmuir cell (Table 3, Eq. 2), where a critical parameter is the fraction of a population that is outside the zone of retention set up by the Langmuir circulation. Smayda (1970) cites Koppen (1921), who suggests that the fraction of mixed-layer plankton entrained in the vortex of a vertical convection cell can be approximated by equation (3) (Table 3). This relationship was derived originally by Schmidt (1913) for particles sinking through a turbulent atmosphere and was applied to the development of hailstones. The relationship can be derived by calculating the ratio of areas of two discs of rotation defined by the stream functions of a convection cell and a sinking particle trapped within it. Substitution of equation (3) into equation (2) results in the definition of loss from a vertical convection cell (Eq. 4).

By dividing equation (1) by equation (4) and using typical values for the parameters, we can examine the relationship between sinking losses within a convection cell and in the absence of such water movement (Eq. 5, Table 3). With a mixed layer depth of 10–20 m, upwelling speeds of 10 $m \cdot d^{-1}$ (typical maximum speeds from the transect model), and a loss rate from the zone of retention of 0.02 d^{-1}, we obtain results similar to those of Titman and Kilham (1976) for Langmuir cells. That is, if the same sinking rate were used in equations (1) and (4), the algebraic loss rate (L_s) would be 10–30 times greater than that calculated as loss from a convection cell (L_c). Also, under the above conditions, to affect similar loss rates in both contexts, the sinking rate used in equation (1) (i.e. one-dimensional models) must be $\frac{1}{10}$ – $\frac{1}{30}$ that used in equation (2).

The final test of the hypothesis that unrealistic sink-

TABLE 1. Ranges of sinking rates of algae of sizes typical of Lake Ontario plankton.

Rate ($m \cdot d^{-1}$)	Comment	Reference
0.2–0.5	Marine unicellular, size based on cell diameter	Smayda 1970
0.2–1.4	Marine chains, size based on cell diameter	
0.1–2.0	All cells (marine), size based on surface area to volume ratio	
0.1–1.0	Marine discs, size based on surface area to volume ratio	
0.17–1.7	Marine, sized based on cell volume	Vinogradova 1977
0.26–1.04	*Scenedesmus quadricauda*	Titman 1975
1.26	*Tabellaria fenestrata*	Titman and Kilham 1976
0.1–1.5	*Asterionella formosa*	
0.08–0.24	*Cyclotella meneghiniana*	
0.67–1.87	*Melosira agassizii*	

TABLE 2. Plankton sinking rates used in Great Lakes' models.

Lake/Bay	Rate ($m \cdot d^{-1}$)	Reference
Grand Traverse Bay	0.02–0.05	Canale et al. 1976
Saginaw Bay	0.05	Bierman et al. 1979
Lake Ontario	0.03–0.05	Scavia 1980
Lake Ontario	0.1	Thomann et al. 1975
Lake Erie	0.05	DiToro and Connolly 1979
Saginaw Bay–Lake Huron	0.05	DiToro and Matystik 1979

TABLE 3. Equations[a] comparing sinking losses calculated as simple algebraic loss and as loss from a convection cell.

(1) $L_s = v/Z$

(2) $L_c = D \cdot f$

(3) $1 - f = (1 - v/V)^2$

(4) $L_c = D\frac{v}{V}\left(2 - \frac{v}{V}\right)$

(5) $\frac{L_c}{L_s} = \frac{ZD}{V}\left(2 - \frac{v}{V}\right)$

[a] L_s = algebraic sinking loss, L_c = sinking loss from convection cell, v = sinking rate, Z = mixed-layer depth, V = upwelling speed, D = loss rate from convection cell, f = fraction of area (volume) outside zone of retention for a particle sinking in a convection cell.

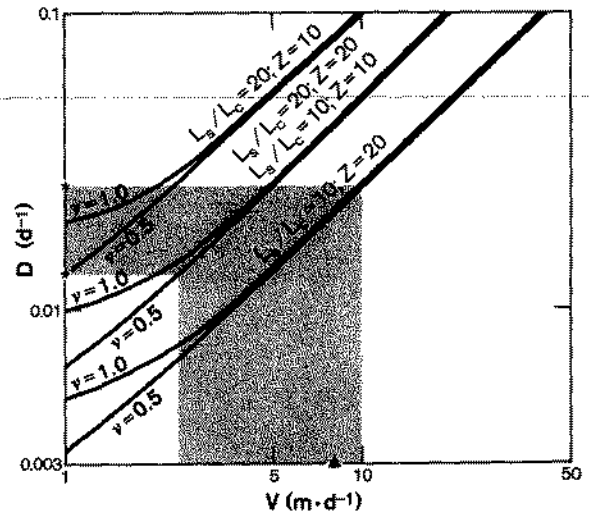

FIG. 8. Plot of turbulent mixing coefficient (D) versus upwelling speed (V) for various values of the ratio L_s/L_c, the mixed layer depth (Z), and sinking speed (v). Asterisks (*) define the range of D from Lake Ontario dye experiments. The solid triangle represents typical upwelling speeds calculated in the model.

ing rates in one-dimensional models are a result of the need to parameterize the effects of water circulation is to determine if the required horizontal loss rate of 0.02 d^{-1} is reasonable for the scales under consideration. Kullenberg et al. (1973) performed dye experiments in Lake Ontario to estimate coefficients of turbulent mixing. They reported horizontal diffusivities for both the region of the epilimnion and the region of the thermocline and the hypolimnion. These diffusivities, divided by the square of the mixing lengths (3–10 km) under consideration, are a rough estimate of the horizontal loss rate. These calculations result in values of D (d^{-1}) between 0.013 and 0.026; thus, a value of 0.02 d^{-1} is reasonable. The relationship between L_c and L_s in terms of D and V, from equation (5), is shown in Fig. 8. Here we examine specifically the case of one-dimensional versus two-dimensional models of Lake Ontario; thus, we know sinking rates were increased from 0.05 to 0.5 $m \cdot d^{-1}$, respectively. If the rates were not adjusted, we would expect an L_s:L_c ratio of about 12:1 (Eq. 5, Table 3). In Fig. 8 we plot D versus V for L_s/L_c = 10 and 20, and Z and v relevant to Lake Ontario. It can be seen that to obtain correct L_s/L_c ratios with appropriate values of v and Z and with D from Kullenberg et al. (1973), upwelling speeds (V) would have had to have been 2–10 $m \cdot d^{-1}$. This is the range of values obtained during our two-dimensional simulations.

From this analysis we suggest that reduced sinking rates are required in one-dimensional models of the Great Lakes partially because entrainment of phytoplankton in large-scale circulation, in a fashion similar to entrainment in Langmuir cells, effectively reduces their overall loss rate.

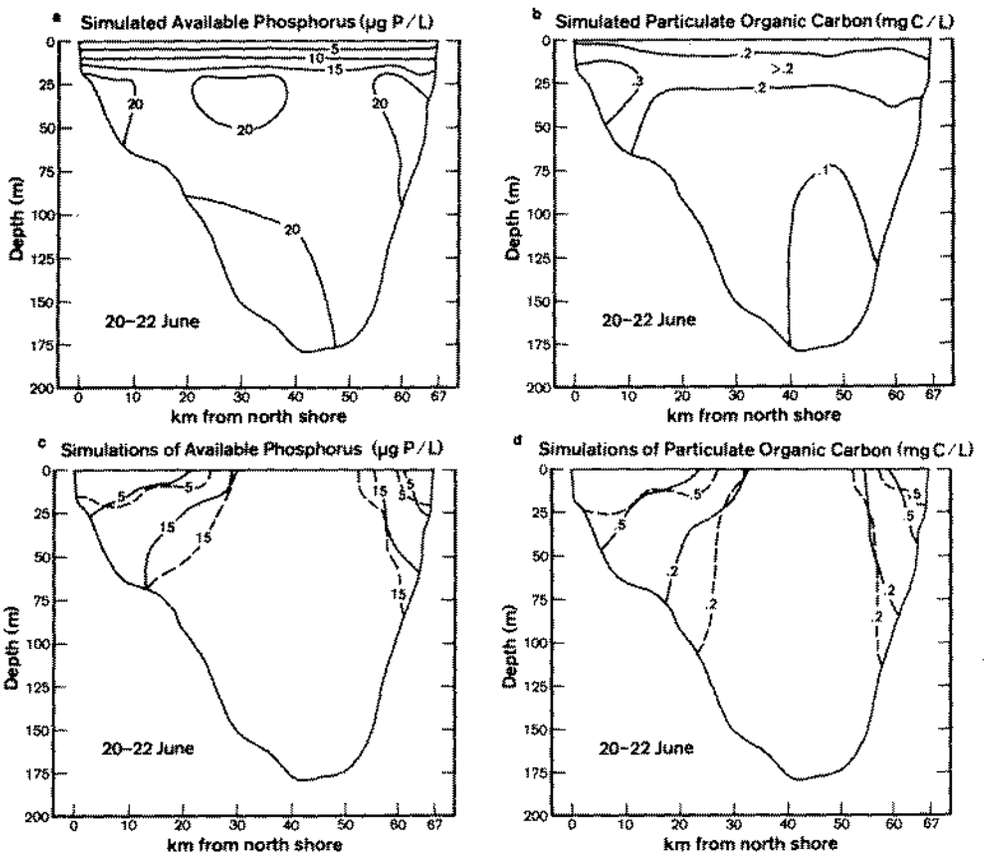

FIG. 9. Contours of model output demonstrating the relative effects of physical and biological processes on the distributions of available phosphorus (μg P/L) and particulate organic carbon (mg C/L). a, b — contours of model output generated with no advection or diffusion included; c, d — broken lines represent normal case (i.e. all processes included); solid lines represent simulation without vertical or horizontal advection.

HYDRODYNAMIC TRANSPORT VERSUS IN SITU PRODUCTION

During spring there are several physical mechanisms that influence the distribution of chemical and biological parameters. Differences in surface temperature can stimulate different rates of biomass production and nutrient cycling. Differences in vertical temperature gradients can produce different intensities of vertical mixing. Currents driven by density differences or wind stress can bring nutrients into the photic zone.

Munawar and Munawar (1975) suggest that vertical mixing is the most important physical mechanism in determining the distribution of diatoms in the nearshore region of Lake Ontario. Menon et al. (1971) found more bacteria on the shore side of the 4° isotherm, but did not suggest a reason. Gachter et al. (1974) explained that differences in offshore versus inshore nutrient concentrations in Lake Ontario were due to deep vertical mixing in the offshore water.

We performed some numerical experiments to find out which of the physical mechanisms was most important. In these experiments we ran two simulations and compared the results to the original calculations discussed above (henceforth, the normal case). In the first simulation, we eliminated mass transport by advection and diffusion. In the second simulation, only vertical diffusion was included. In all cases in situ biological and chemical processes and sinking were included and temperature distributions were kept the same as in the normal case. The results of these experiments are summarized in Fig. 9 for available phosphorus and particulate organic carbon.

The simulation with no advection or diffusion showed that phytoplankton production in the cold offshore waters, although reduced when compared to inshore waters, is sufficient to deplete nutrients from the surface layer within the 72-d simulation (Fig. 9a) Therefore, temperature-controlled, in situ production alone was not sufficient to produce the persistent offshore gradients. Also evident in this experiment (Fig. 9b) were plankton concentration peaks in the second model layer (10–20 m) rather than in the surface layer, as in the normal simulations and in the observations. Depth pro-

files such as these are typical of lakes that experience little turbulence (e.g. Hutchinson 1967, p. 286).

The second simulation illustrates that vertical mixing, together with in situ production, is sufficient to reproduce the observed biological and chemical patterns. The major effect of vertical and horizontal advection is to smooth the nutrient gradients through increased mixing caused by repeated reversals in flow direction. The same was true for plankton along the relatively dilute, cold-water boundary (Fig. 9d).

It appears that the distribution of chemical and biological properties in the vicinity of the 4° isotherm is controlled primarily by the interaction of in situ processes and the differences in vertical mixing on either side of the isotherm. Shoreward, the water mass is weakly stratified vertically. This reduces the mixed depth and allows increased biomass production and subsequent nutrient depletion (Sverdrup 1953; Stadelmann et al. 1974). Lakeward, deep vertical mixing keeps a significant portion of the phytoplankton removed from the sunlit surface layers and therefore inhibits their growth.

ATWATER, M. A., AND J. T. BALL. 1974. The radiation and cloud cover for Lake Ontario during IFYGL. Final Rep. 4: 130–513a, contract 2-35353, Center for the Environment and Man, Hartford, CT. 111 p.

BENNETT, J. R. 1971. Thermally driven lake currents during the spring and fall transition periods, p. 535–544. *In* Proc. 14th conf. Great Lakes Res., Ann Arbor, MI.

1974. On the dynamics of wind-driven lake currents. J. Phys. Oceanogr. 4: 400–414.

BIERMAN, V. I., E. F. STOERMER, J. E. GANNON, AND V. E. SMITH. 1979. The development and calibration of a multiclass, internal pool, phytoplankton model for Saginaw Bay, Lake Huron. Ecological Research Series, U.S. Environmental Protection Agency, Duluth, MN. (In press)

BOYCE, F. M. 1975. Heat content of Lake Ontario and estimates of average surface fluxes during IFYGL. Manuscript report, Canada Centre for Inland Waters, Burlington, Ont.

CANALE, R. P., L. M. DEPALMA, AND A. H. VOGEL. 1976. A plankton-based food wed model for Lake Michigan, p. 33–74. *In* R. P. Canale [ed.] Modeling biochemical processes in aquatic ecosystems. Ann Arbor Science, Ann Arbor, MI.

DITORO, D. M., AND J. CONNOLLY. 1979. Mathematical models of water quality in large lakes. Part II: Lake Erie. Ecological Research Series, U.S. Environmental Protection Agency, Duluth, MN. (In press)

DITORO, D. M., AND W. F. MATYSTIK JR. 1979. Mathematical models of water quality in large lakes. Part I: Lake Huron and Saginaw Bay. Model development, verification, and simulations. Ecological Research Series, U.S. Environmental Protection Agency, Duluth, MN. (In press)

EPPLEY, R. W., R. W. HOLMES, AND J. D. H. STRICKLAND. 1967. Sinking rates of marine phytoplankton measured with a fluorometer. J. Exp. Mar. Biol. Ecol. 1: 191–208.

GACHTER, R., R. A. VOLLENWEIDER, AND W. A. GLOOSCHENKO. 1974. Seasonal variations of temperature and nutrients in the surface waters of Lakes Ontario and Erie. J. Fish. Res. Board Can. 31: 275–290.

HUTCHINSON, G. E. 1967. A treatise on limnology. Vol. 2. Introduction to lake biology and the limnoplankton. Wiley, New York. 1115 p.

KOPPEN, W. 1921. Das schweben das planktons. Ann. Hydrogr. Berl. 49: 170–173.

KULLENBERG, G., C. R. MURTHY, AND H. WESTERBERG. 1973. An experimental study of diffusion characteristics in the thermocline and hypolimnion regions of Lake Ontario, p. 774–790. *In* Proc. 16th Conf. Great Lakes Res., Ann Arbor, MI.

MCNOWN, J. S., AND J. MALAIKA. 1950. Effects of particle shape on settling velocity at low Reynolds numbers. Trans. Am. Geophys. Union 31: 74–82.

MENON, A. S., B. J. DUTKA, AND A. A. JURKOVIC. 1971. Preliminary bacteriological investigation of the Lake Ontario thermal bar, p. 59–68. *In* 14th Conf. Great Lakes Res., Ann Arbor, MI.

MUNAWAR, M., AND I. F. MUNAWAR. 1975. Some observations on the growth of diatoms in Lake Ontario with emphasis on *Melosira binderana* Kutz during thermal bar conditions. Arch. Hydrobiol. 75: 490–499.

SCAVIA, D. 1980. An ecological model of Lake Ontario. Ecol. Model. 8: 49–78.

1979. Examination of phosphorus cycling and control of phytoplankton dynamics in Lake Ontario with an ecological model. J. Fish. Res. Board Can. 36: 1336–1346.

SCAVIA, D., B. J. EADIE, AND A. ROBERTSON. 1976. An ecological model for Lake Ontario — model formulation, calibration and preliminary evaluation. NOAA Tech. Rep. ERL 371-GLERL 12: 63 p.

SCHMIDT, W. 1913. Schweben von teilchen in luftwirbeln. Meteorol. Z. p. 171–174.

SIMONS, T. J. 1976a. Analysis and simulation of spatial variations of physical and biochemical process in Lake Ontario. J. Great Lakes Res. 2: 215–233.

1976b. Verification of numerical models of Lake Ontario III. Long-term heat transports. J. Phys. Oceanogr. 19: 628–635.

SMAYDA, T. J. 1970. The suspension and sinking of phytoplankton in the sea. Oceanogr. Mar. Biol. Ann. Rev. 8: 353–414.

1974. Some experiments on the sinking characteristics of two freshwater diatoms. Limnol. Oceanogr. 19: 628–635.

STADELMANN, P., AND A. FRASER. 1974. Phosphorus and nitrogen cycle on a transect in Lake Ontario during the International Field Year 1972–1973 (IFYGL), p. 92–107. *In* Proc. 17th Conf. Great Lakes Res., Ann Arbor, MI.

STADELMANN, P., J. E. MOORE, AND E. PICKETT. 1974. Primary productivity in relation to temperature structure, biomass concentration, and light conditions at an inshore and offshore station in Lake Ontario. J. Fish. Res. Board Can. 31: 1215–1232.

STADELMANN, P., AND M. MUNAWAR. 1974. Biomass parameters and primary production at a nearshore and a midlake station of Lake Ontario during IFYGL, p. 109–119. *In* Proc. 17th Conf. Great Lakes Res., Ann Arbor, MI.

STEELE, J. H. 1965. Notes on some theoretical problems in production ecology, p. 383–398. *In* C. R. Goldman [ed.] Primary production in aquatic environments. Univ. of Calif. Press, Univ. of Calif., Berkeley, CA.

STOERMER, E. F., AND T. B. LADEWSKI. 1978. Phytoplankton associations in Lake Ontario during IFYGL. Spec. Rep. 62, Great Lakes Res. Division, Univ. Mich., Ann Arbor, MI, 106 p.

STOMMEL, H. 1949. Trajectories of small bodies sinking slowly through convection cells. J. Mar. Res. 8: 24–29.

SVERDRUP, H. U. 1953. On conditions for the vernal blooming of phytoplankton. J. Cons. Perm. Int. Exp. Mer 18: 278–295.

THOMANN, R. U., D. M. DITORO, R. P. WINFIELD, AND D. J. O'CONNOR. 1975. Mathematical modeling of phytoplankton in Lake Ontario. Part 1: Model development and verification. Ecological Research Series, U.S. Environmental Protection Agency, EPA-660/3-75-005, Corvallis, OR. 177 p.

TITMAN, D. 1975. A fluorometric technique for measuring sinking rates of freshwater phytoplankton. Limnol. Oceanogr. 20: 869–875.

TITMAN, D., AND P. KILHAM. 1976. Sinking in freshwater phytoplankton: some ecological implications of cell nutrient status and physical mixing processes. Limnol. Oceanogr. 21: 409–417.

VINOGRADOVA, L. A. 1977. Experimental determination of the gravitational sinking rate of marine planktonic algae. Oceanology 17: 458–461.

VOLLENWEIDER, R. A. 1965. Calculation models of photosynthesis — depth curves and some implications regarding day rate estimates in primary production measurements, p. 425–457. *In* C. R. Goldman [ed.] Primary productivity in aquatic environments. Univ. of Calif. Press, Univ. of Calif., Berkeley, CA.

VOLLENWEIDER, R. A., M. MUNAWAR, AND P. STADELMANN. 1974. A comparative review of phytoplankton and primary production in the Laurentian Great Lakes. J. Fish. Res. Board Can. 31: 739–762.